# The TREK-1 potassium channel is involved in both the analgesic and anti-proliferative effects of riluzole in bone cancer pain

Mélissa Delanne-Cuménal, Sylvain Lamoine, Mathieu Meleine, Youssef Aissouni, Laetitia Prival, Mathilde Fereyrolles, Julie Barbier, Christine Cercy, Ludivine Boudieu, Julien Schopp, et al.

Biomedicine & Pharmacotherapy 176 (2024) 116887

Contents lists available at ScienceDirect

Biomedicine & Pharmacotherapy

journal homepage: www.elsevier.com/locate/biopha

# The TREK-1 potassium channel is involved in both the analgesic and anti-proliferative effects of riluzole in bone cancer pain

Mélissa Delanne-Cuménal [a], Sylvain Lamoine [a], Mathieu Meleine [a], Youssef Aissouni [a], Laetitia Prival [a], Mathilde Fereyrolles [a], Julie Barbier [a], Christine Cercy [a], Ludivine Boudieu [a], Julien Schopp [a], Michel Lazdunski [c,d], Alain Eschalier [a,b], Stéphane Lolignier [a], Jérôme Busserolles [a,*]

[a] Université Clermont Auvergne, Inserm, CHU Clermont-Ferrand, Neuro-Dol, Clermont-Ferrand F63000, France
[b] Institut Analgesia, Faculté de Médecine, BP38, Clermont-Ferrand 63001, France
[c] Université de Nice Sophia Antipolis, Valbonne 06560, France
[d] CNRS, Institut de Pharmacologie Moléculaire et Cellulaire, UMR 7275, 660 Route des Lucioles Sophia Antipolis, Valbonne 06560, France

ARTICLE INFO

*Keywords:*
Bone cancer pain
TREK-1 potassium channel
Prostate cancer
Riluzole

ABSTRACT

*Background:* The metastasis of tumors into bone tissue typically leads to intractable pain that is both very disabling and particularly difficult to manage. We investigated here whether riluzole could have beneficial effects for the treatment of prostate cancer-induced bone pain and how it could influence the development of bone metastasis.

*Methods:* We used a bone pain model induced by intratibial injection of human PC3 prostate cancer cells into male SCID mice treated or not with riluzole administered in drinking water. We also used riluzole *in vitro* to assess its possible effect on PC3 cell viability and functionality, using patch-clamp.

*Results:* Riluzole had a significant preventive effect on both evoked and spontaneous pain involving the TREK-1 potassium channel. Riluzole did not interfere with PC3-induced bone loss or bone remodeling *in vivo*. It also significantly decreased PC3 cell viability *in vitro*. The antiproliferative effect of riluzole is correlated with a TREK-1-dependent membrane hyperpolarization in these cells.

*Conclusion:* The present data suggest that riluzole could be very useful to manage evoked and spontaneous hypersensitivity in cancer-induced bone pain and has no significant adverse effect on cancer progression.

## 1. Introduction

Bone metastases are a common complication of cancer and occur in 65–80 % of patients with metastatic breast and prostate cancers [1]. The metastasis of tumors into bone tissue typically leads to intractable pain that is both very disabling and particularly difficult to manage [2]. The difficulty is in part due to the multifactorial nature of this particular pain, which combines nociceptive and neuropathic components. At present, opioids are the only pharmacological treatment available [3–5]. However, they are unfortunately limited in their efficacy [6]. The beneficial effects of opioids in other models of pain are largely due to opening of the TREK-1 channels, a class of $K^+$ channels [7]. TREK1 is a unique type of ionic channels: it is a background $K^+$ channel [8], a mechanosensitive K+ channel [8], and a channel that is also highly sensitive to thermal variations [9]. It is a major player in polymodal pain perception [10,11].

Riluzole, a drug that has long been on the clinical market to treat (nearly) all patients suffering from amyotrophic lateral sclerosis, is an activator of the TREK-1 channel [12] and exerts a potent analgesic effect in several models of inflammatory and neuropathic pain [13–17]. Interestingly, riluzole also has anti-proliferative effects [18]. For all these reasons, and because of the urgent need to find new treatments for pain associated with bone cancer, we decided to analyze the effects of riluzole on prostate cancer-induced bone pain. We used a bone cancer pain model induced by intratibial injection of human PC3 prostate cancer cells into immunodeficient SCID mice, and administered riluzole in drinking water. In this model, riluzole had a significant analgesic effect involving, as expected, activation of the TREK-1 potassium

* Correspondence to: U1107, Neuro-Dol, Faculty of Medicine, 28, pl. H.Dunant, Clermont-Ferrand 63000, France.
*E-mail address:* jerome.busserolles@uca.fr (J. Busserolles).

https://doi.org/10.1016/j.biopha.2024.116887
Received 19 April 2024; Received in revised form 3 June 2024; Accepted 3 June 2024
Available online 8 June 2024

channel. In addition, riluzole treatment has also been observed to significantly decrease prostate cancer (PCa) cell viability *in vitro*. This antiproliferative effect of riluzole also involves an increase in the expression of TREK-1 channels in cancer cells.

## 2. Methods

### 2.1. Animals

All experiments were performed on 5-week-old severe combined immunodeficient (SCID) male mice provided by Janvier (France), kept on a 12 h light/dark cycle with food and water ad libitum. Behavioral experiments were performed blind to the treatment in a quiet room by the same experimenter for a given test who took great care to minimize or avoid discomfort of the animals. All animal procedures were approved by the local animal ethics committee (APAFIS#3773) and experiments were performed according to the European Union guidelines for the care and use of animals (Directive 2010/63/EU). Animals bearing tumor xenografts were carefully monitored for established signs of distress and discomfort and were humanely euthanized.

### 2.2. Intramedullary implantation of metastatic prostate cancer cells

For intra-osseous tumor xenograft experiments in SCID mice, a small hole was drilled under anesthesia with a 26-gauge sterile needle through the left tibia with the knee flexed. Using a new sterile needle fitted to a 50-µl sterile Hamilton syringe (Hamilton Co, Bonaduz, GR, Switzerland), a suspension of PC3 cells ($5 \times 10^5$ in 10 µL PBS) was carefully injected into the bone marrow cavity as previously described [19]. Animals were euthanized after 5 weeks of experimentation.

### 2.3. Behavioral tests

#### 2.3.1. Von Frey test

Mechanical sensitivity was assessed with a calibrated Von Frey filament of 0.6 g. The filaments were applied perpendicularly to the plantar surface of the hind paw and pressed until they bent. Five stimuli per hind paw were applied at intervals of 3–5 s and the total number of responses was measured.

#### 2.3.2. Static weight bearing (SWB)

The incapacitance test (bioseb, Boulogne, France) was used to evaluate spontaneous pain. During this test, the mouse is placed in a holder (after one week of acclimatization) and comfortably maintained in a rearing position while its hind paws are placed on two sensor plates. According to the degree of pain, the animal adjusts its weight distribution on the two rear paws. The results are expressed as a percentage of weight distribution on the ipsilateral paw. An animal with a balanced posture will therefore have a weight distribution of 50 %, and a decrease in this value will be a sign of the appearance of pain that forces the animal to transfer weight to its valid paw.

### 2.4. Pharmacological treatments

The two drugs used were riluzole (Tocris), and the TREK-1 blocker spadin (Tocris). All solutions were prepared extemporaneously in 0.9 % (w/v) NaCl solution for spadin and in the drinking water for riluzole.

We chose to administrate riluzole in the drinking water to minimize the stress associated with repeated gavage or daily injections. We added riluzole in drinking water at 60 µg/mL, as described previously [13]. We measured the water consumption of SCID mice treated or not with spadin and riluzole (n = 6 per group) twice a week by weighing their bottles. This allowed us to estimate the average riluzole dose ingested to be 13.2 mg/kg/day. The mean water consumption for the study was not significantly different between the groups (2.02 ± 0.27 mL/mouse for the sham group, 2.11 ± 0.45 mL/mouse for the PC3 group, 1.77 ± 0.05 mL/mouse for the riluzole group, 1.94 ± 0.01 mL/mouse for the spadin group, and 1.77 ± 0.05 mL/mouse for the riluzole + spadin group).

### 2.5. In vivo imaging

All imaging experiments were performed by the Molecular Imaging and Theranostic Strategies (iMost) group, UMR 1240 Inserm/UCA in Clermont-Ferrand, France. All animals were imaged by SPECT/CT with a 99mTc-HMDP radiotracer. Ten MBq of 99mTc-hydroxymethylene diphosphonate (99mTc-HMDP, Osteocys; Dupharma A/S, Kastrup, Denmark) per mouse were intraperitoneally injected to evaluate bone alterations at D14, D21, D28 and D35 post-PC3 intratibial injection. Two and a half hours later, planar acquisition was performed for 5 minutes (15 % window at 140 keV) on the animal positioned in ventral decubitus on a parallel collimator (20 mm/1.8/0.2) of a gamma camera for small animals (γImager, Biospace) under isoflurane anesthesia (1 %).

Quantitative analysis of scintigrams was performed with GammaVision+ software (Biospace) using fixed-sized rectangular regions of interest (ROIs) on the hind paws. For each time point and each animal, the bone scan ratio was calculated using the following equation: ratio = pathological paw average activity (Bq)/contralateral paw average activity (Bq).

### 2.6. Cell culture and viability

The human PC3 prostate cancer cells (ATCC, ATCC® CRL-1435™) were cultured in Nutrient Mixture F-12 (DMEM/F-12) at 37 °C in a humidified atmosphere of 95 % air/5 % $CO_2$. The culture medium was supplemented with 10 % (v/v) heat-inactivated fetal bovine serum (FBS) and 1 % of a 100 × penicillin/streptomycin solution. Drugs used were dissolved in 100 % DMSO. The treatments were performed so that the final concentration of DMSO did not exceed 0.4 %.

3-(4,5-Dimethylthiazol-2-yl)-2,5-diphenyltetrazolium bromide (MTT) assay was performed according to the manufacturer's protocol (Life Technologies). Briefly, $7.5 \times 10^3$ cells were plated in a 96-well plate and treated for 48 h with riluzole and/or spadin as indicated. Quantification of the MTT assay was performed using an epoch microplate spectrophotometer (Biotek Instruments, Inc., Winooski, VT). The absorbance of vehicle-treated wells (not exceeding 0.4 %DMSO) was designated as 100 % and cell survival expressed as a percentage of this value. Data shown represent the mean ± SEM of three independent experiments performed in triplicate.

### 2.7. Cell functional assays

#### 2.7.1. Patch-clamp

PC3 cells were seeded in 35 mm diameter Petri dishes 3 days before incubation of the cells with the different treatments (Riluzole 50 µM, Spadin 1 µM, Riluzole 50 µM + Spadin 1 µM or vehicles) for 48 hours. Resting membrane potential (Vm) and current were recorded in whole cell configuration using an Axopatch 200B amplifier (Axon instruments) and digitalized with a Digidata 1440A acquisition interface (Axon Instruments). Clampex 8.2 software was used for recordings and clamping parameters. The recording micropipettes were made by stretching borosilicate capillaries and had a resistance between 1.5 and 2.5 MΩ. The intracellular solution contained (in mM): 130 KCl, 8 NaCl, 1 $MgCl_2$, 1 $CaCl_2$, 4 MgATP, 0.4 NaGTP, 2 EGTA, 10 HEPES (pH 7.35 adjusted with KOH, Osmolarity 310 mOsm adjusted by adding sucrose). The extracellular solution contained (in mM): 140 NaCl, 4 KCl, 2 $CaCl_2$, 1 $MgCl_2$, 5 D-Glucose, 10 HEPES (pH7.4 adjusted with NaOH, Osmolarity 305 mOsm adjusted by adding sucrose). The data obtained were filtered at 1 kHz and recorded at 10 kHz.

#### 2.7.2. Thalium flux assay

FLuxOR Potassium Assay Kit (Thermofisher) was used according to

the manufacturer's protocol. Briefly, $50 \times 10^3$ PC3 cells were plated in a 96-well plate and treated for 48 h with riluzole and/or spadin as indicated. The medium was then removed and replaced with 40 μL of buffer containing a thallium-sensitive fluorescent dye for 1 h at 37 °C. Fluorescence recording was done on a Fexstation3 apparatus using the flex mode (Molecular Devices, San Jose, CA). Baselines were recorded for 20 s before thallium addition. Fluorescence was then monitored for 60 s and the results expressed as ΔF/cell viability, with cell viability being measured by the MTT assay after the thallium flux assay.

### 2.8. Statistical analysis

Statistical significance of differences between groups (data are expressed as mean ± S.E.M.) was tested using the Graphpad software program Version 9.0. The specific tests used and p-value levels are indicated in the figure legends.

## 3. Results

### 3.1. Riluzole decreases mechanical hypersensitivity and spontaneous nocifensive behavior in cancer-induced bone pain (CIBP) mice

We performed intra-osseous tumor xenograft experiments using the human androgen independent AR-negative cell line PC3, which induces pure osteolytic bone metastases in mice [19]. PC3 cells were injected through the right tibia of 5- to 6-week-old anesthetized male SCID mice. We also used a group of mice (n = 6) that were sham-operated. Seven days after injection of PC3 cells, we exposed half of the mice to riluzole

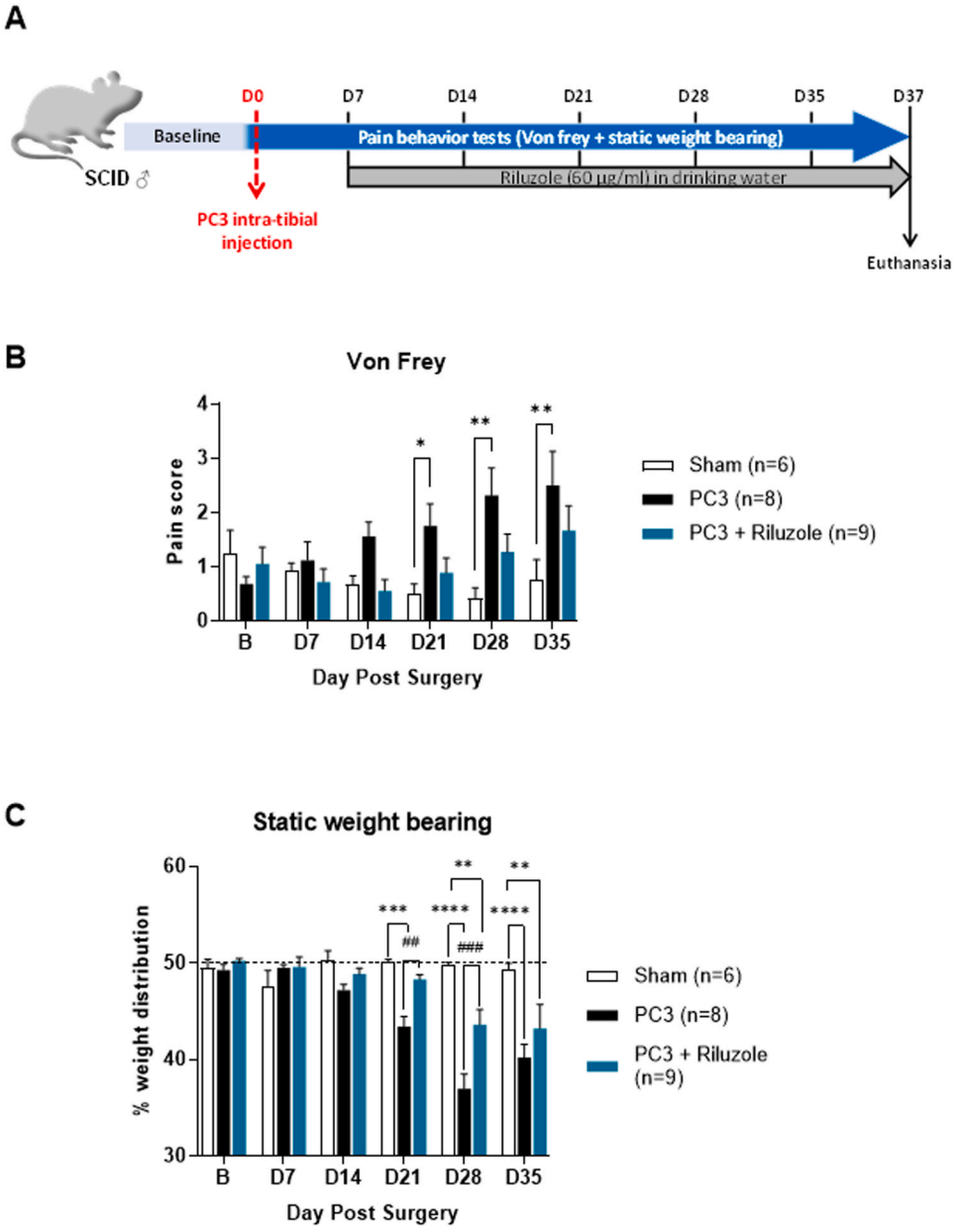


**Fig. 1. Riluzole decreases both mechanical hypersensitivity and spontaneous pain in a murine model of CIBP** (A) Diagram illustrating the experimental protocol for the induction of the CIBP model in SCID mice. (B) Mechanical pain hypersensitivity was assessed by the von Frey test. Pain scores represent the number of paw withdrawals obtained over five stimulations with a 0.6 g filament. (C) Spontaneous pain was assessed by the weight-bearing test. Pain was evaluated by the weight distribution on the ipsilateral paw. Riluzole significantly decreased both mechanical hypersensitivity and spontaneous pain. Values are mean ± SEM (n = 6–9 per group). Statistical analysis was performed using a two-way repeated measure analysis of variance (RM ANOVA) and a Tukey post hoc test; *, $p < 0.05$, **, $p < 0.01$, ***, $p < 0.001$, *versus* the sham group; #, $p < 0.05$, ##, $p < 0.01$, *versus* the PC3 group.

(60 µg/mL p.o. in the drinking water as previously described [13]), up to the end of the study (day 35) (Fig. 1A). We measured water consumption, which translates to an average dose of riluzole of 13.2 mg/kg/day. After correction for the body surface area [20], this corresponds to a dose of 1.07 mg/kg/day in a man, *i.e.* an administration of 85.6 mg/day for a man of 80 kg. Patients with amyotrophic lateral sclerosis (ALS) receive orally 100 mg of riluzole/day.

Mechanical hypersensitivity was established in PC3-injected mice from day 21 after the injection in the paw (Fig. 1B). Riluzole significantly decreased this symptom (two-way repeated measure ANOVA: riluzole F [2, 20] = 5.548, P = 0.0121; time: F [5, 100] = 2.324, P = 0.0484; interaction: F [10, 100] = 2.165, P = 0.026=. Mechanical hypersensitivity also developed in the contralateral paw from day 28 after injection (Supplementary Fig. 1), which could be indicative of central sensitization, and was significantly decreased by riluzole (two-way repeated measure ANOVA: riluzole F [2, 20] = 6.233, P = 0.0079; time: F [5, 100] = 2.538, P = 0.0331; interaction: F [10, 100] = 1.337, P = 0.2216. The analgesic efficacy of riluzole was also assessed in CIBP mice by the static weight-bearing test, which assesses spontaneous nocifensive behavior. PC3 cell-injected animals treated with vehicle manifested increased spontaneous nocifensive behaviors on day 14 that continued for the duration of the experiment (Fig. 1C). Riluzole treatment (60 µg/mL, p.o.) decreased spontaneous pain behavior (two-way repeated measure ANOVA: riluzole F [2, 20] = 21.81, P < 0.0001; time: F [2.429, 48.58] = 15.26, P < 0.0001; interaction: F [10, 100] = 5.574, P < 0.0001. Of note, a group of PC3-injected mice received morphine (3 mg/kg, i.p.) at days 28 and 35 (Supplementary data 2A). In agreement with previous reports [21,22], morphine failed to exert any effect at this dose against spontaneous pain in CIBP mice, neither when assessed at day 28 (two-way repeated measure ANOVA: morphine F [1, 14] = 2.206, P = 0.1596; time: F [1.655, 23.17]= 0.5364, P = 0.5589; interaction: F [2, 28] = 0.3981, P = 0.6754) nor at day 35 (two-way

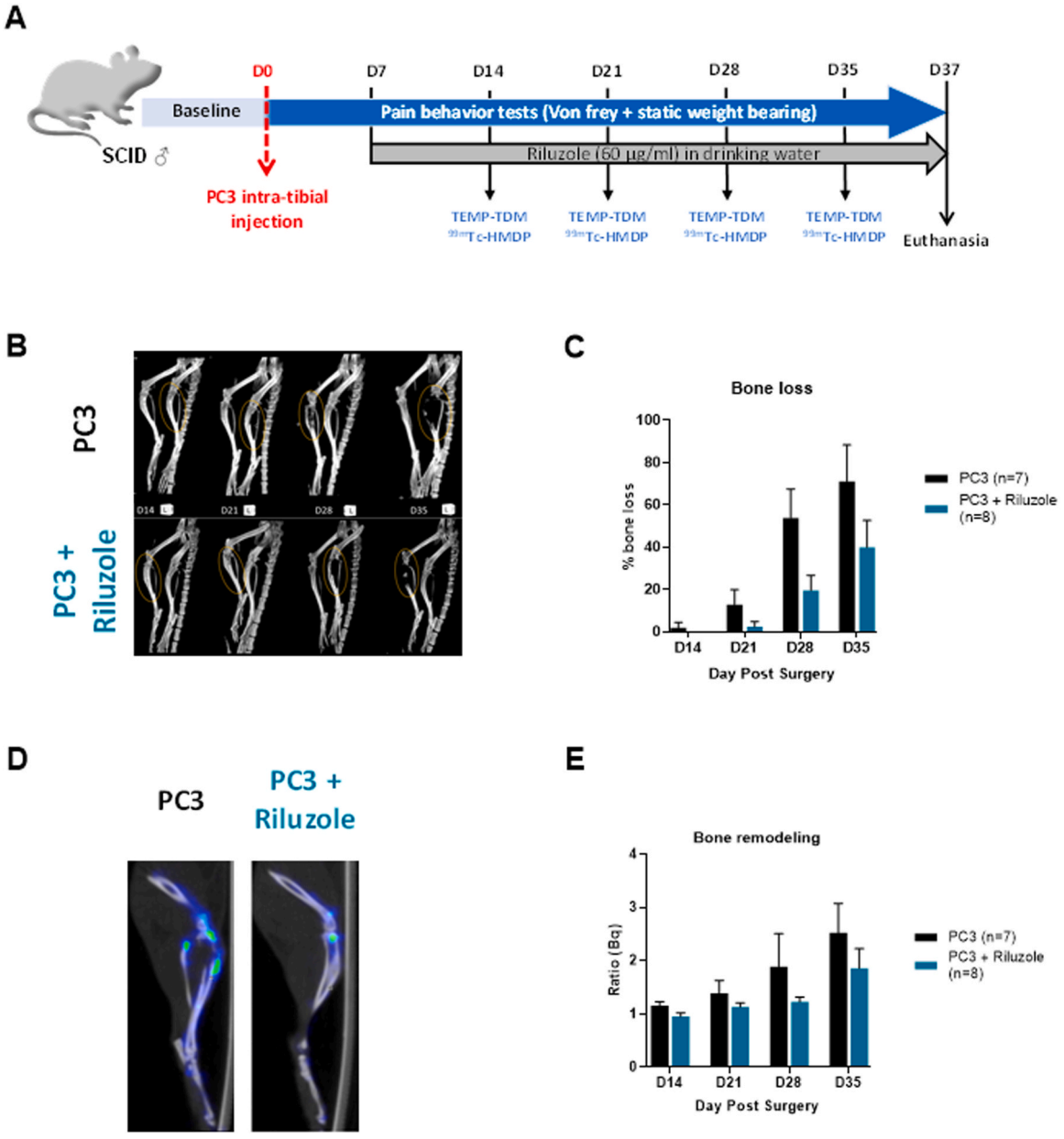


**Fig. 2. Riluzole does not worsen bone loss and bone remodeling in a murine model of CIBP** (A) Diagram illustrating the experimental protocol for riluzole (60 µg/mL p.o in the drinking water) administration in the CIBP model (B) Bone loss was measured with µCT images. (C) Bone remodeling was measured by bone scintigraphy using the osteoarticular radiotracer 99mTc-HMDP. Riluzole does not significantly affect bone loss nor bone remodeling induced by PC3 injection. Values are mean ± SEM (n = 7–8 per group). Statistical analysis was performed with a two-way repeated measure analysis of variance (RM ANOVA).

repeated measure ANOVA: morphine F(1, 14) = 0.8444, P = 0.3737; time: F [1.772, 24.80] = 1.937, P = 0.1688; interaction: F [2, 28] = 3.909, P = 0.0318). In contrast, the same dose has proved efficient in inflammatory pain models [21,23].

### 3.2. Riluzole does not worsen PC3-induced bone loss or bone remodeling in vivo

Prostate cancer cells that spread out of the prostate show an exquisite tropism for the bone. The growth of prostate cancer cells alters bone remodeling (formation and resorption) by secreting factors that will directly affect osteoblasts (bone-forming cells) and osteoclasts (bone-resorbing cells). The interaction between tumor cells with osteoblasts and osteoclasts elicits an osteolytic, osteoblastic, or mixed bone response [24]. A preferential osteolytic response, as modelized here, is characterized by the destruction of normal bone attributable to the occurrence of osteoblast inactivation and osteoclast recruitment and activation in the tumor bone microenvironment. It has been shown that human osteoblasts express TREK-1 mRNA and protein. It has also been hypothesized that TREK-1 has a role in mechanotransduction, leading to bone remodeling [25]. We thus assessed the effect of the drug on both cancer-induced bone loss and bone remodeling. Bone loss, as measured in vivo by μCT, increased from 20 % at day 21 to more than 70 % at day 35 in the PC3 group. No significant effect of riluzole was found regarding this parameter (two-way repeated measure ANOVA: riluzole F [1,9] = 4.633, P = 0.0598; time: F [1.196, 10.76] = 23.74 P = 0.0004; interaction: F [3,27] = 1.962, P= 0.1435). (Fig. 2B–C). Bone remodeling started to increase in parallel at day 21 post-injection and was 2.5-fold significantly higher at day 35 (Fig. 2D-E). Riluzole did not significantly affect this parameter (two-way repeated measure ANOVA: riluzole F [1, 11] = 1.792, P = 0.2077; time: F [1.995, 21.94] = 7.848, P = 0.0027; interaction: F [3, 33] = 0.4997, P = 0.6851).

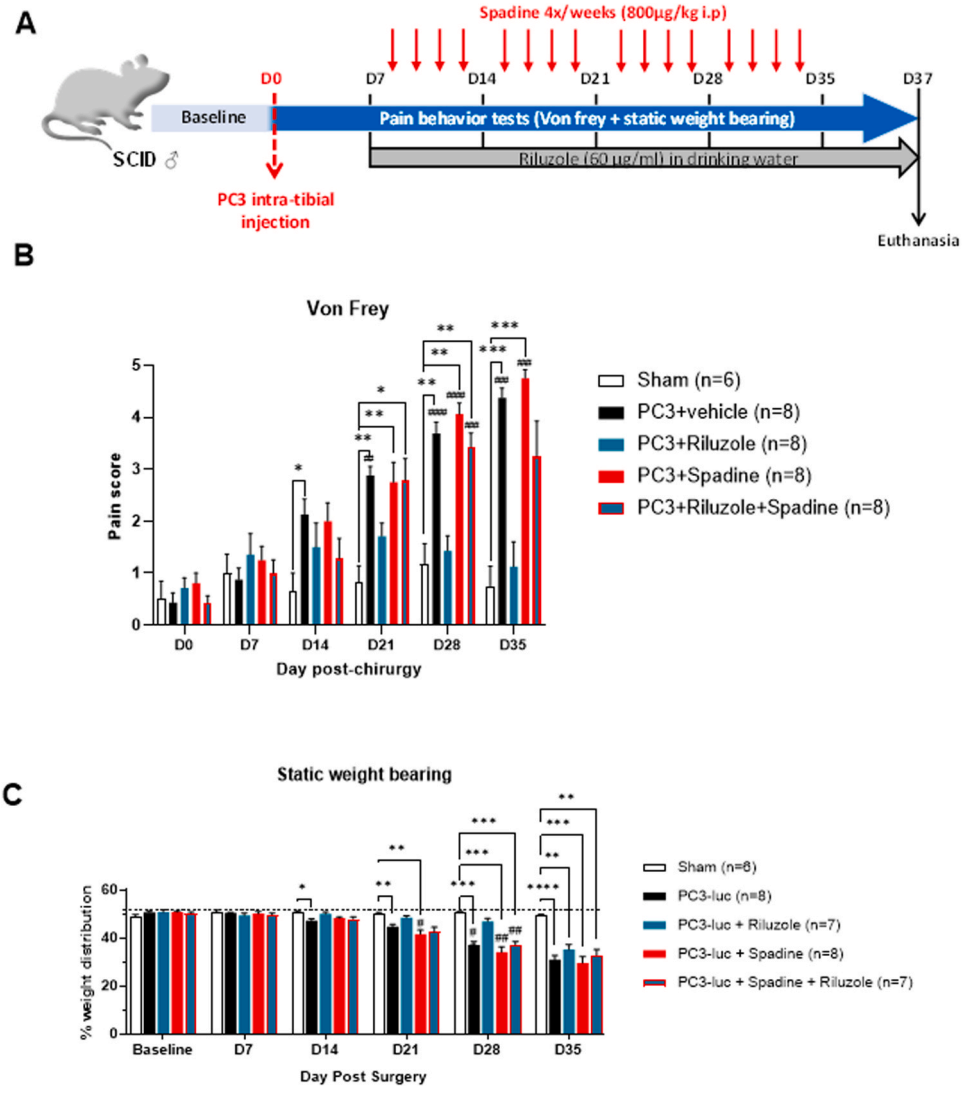


**Fig. 3. The effect of riluzole on bone pain development in CIBP mice involves the TREK-1 channel** (A) PC3 cells were injected through the right tibia of 5- to 6-week-old anesthetized male SCID mice. Seven days after injection of PC3 cells, we exposed half of the mice to riluzole (60 μg/mL in the drinking water) from day 7 to day 35. In half of the mice from each of these two groups, we injected the TREK-1 blocker spadin (800 μg/kg, i.p.) 4 days per week. We also used a group of mice (n = 6) that were sham-operated. (B) Mechanical pain hypersensitivity was assessed by the von Frey test. (C) Spontaneous pain was assessed by the static weight-bearing test. Irrespective of whether the von Frey or static weight-bearing were used, the pharmacological blockade of TREK-1 significantly counteracted the beneficial effect of riluzole. Values are mean ± SEM (n = 6–8 per group). Statistical analysis was performed with a two-way repeated measure analysis of variance (RM ANOVA) and a Tukey post hoc test; *, $p < 0.05$, **, $p < 0.01$, ***, $p < 0.001$, *versus* the sham group; #, $p < 0.05$, ##, $p < 0.01$, ###, $p < 0.001$, *versus* the PC3 group, °, $p < 0.05$, °°, $p < 0.01$, °°°, $p < 0.001$, *versus* the PC3 + riluzole group.

### 3.3. The analgesic effect of riluzole involves the activation of the $K_2P$ ion channel TREK-1 in CIBP mice

We had previously observed that riluzole prevents both sensory and motor deficits induced by cumulative doses of the chemotherapeutic drug oxaliplatin. All the beneficial effects were due to the riluzole action on the TREK-1 potassium channel [13]. We wondered if TREK-1 could also be involved in the therapeutic effect of riluzole in CIBP. To test this hypothesis, PC3 cells were injected through the right tibia of 5- to 6-week-old anesthetized male SCID mice. Seven days after injection of PC3 cells, we exposed half of the mice to riluzole (60 μg/mL in the drinking water) from day 7 to day 35. In half of the mice from each of these two groups, we injected the TREK-1 blocker spadin (800 μg/kg, i.p.) four days per week. We also used a group of mice (n = 6) that were sham-operated. (Fig. 3A) [26]. Blocking TREK-1 effectively reversed the beneficial effects observed on both mechanical hypersensitivity (two--way repeated measure ANOVA: treatment F [4, 61] = 17.44, P < 0.0001; time: F [4.148, 229.8]= 40.48, P < 0.0001; interaction: F [20, 277]= 5.435, P < 0.0001) (Fig. 3B) and spontaneous nocifensive behavior in CIBP mice (two-way repeated measure ANOVA: treatment F [4, 29] = 41.09, P < 0.0001; time: F [2.439, 70.72]= 98.40, P < 0.0001; interaction: F [20, 145] = 7.785, P < 0.0001) (Fig. 3C).

### 3.4. Riluzole decreases PC3 cell viability in vitro. This effect is correlated with increased hyperpolarization and $K^+$ flux in these cells and involves TREK-1 channels

Riluzole has recently been indicated to slow down cancer cell proliferation and/or to induce cancer cell death. It was effective as an anti-neoplastic drug in cancers of various tissue origins, including skin, breast, pancreas, colon, liver, bone, brain, lung and nasopharynx (for review see [18]). In accordance with the bibliographic data showing an antiproliferative effect of riluzole on many cancer cell lines [27], including prostate cancer (PCa) lines [28,29], we found a dose-dependent negative effect of riluzole on metastatic androgen-independent PC3 cell viability (Fig. 4A). This effect was partially but significantly lost when we applied the selective TREK-1 blocker spadin (Fig. 4B), which *per se* did not affect PC3 cell viability (Suppl. Fig. 3A), suggesting the involvement of TREK-1.

A relation between cancer cell proliferation and resting membrane potential (Vm) was first proposed in 1971 by Cone and has since been backed up by many studies [30]. Highly proliferative tumor cells generally have a depolarized Vm, whereas quiescent cells are hyperpolarized [31]. In accordance with these results, using patch-clamp we found PC3 Vm to be around −30 mV. When applied for 48 h, riluzole significantly decreased PC3 cell Vm to − 47.7 +/- 5.24 mV (Fig. 4C). Both the selective TREK-1 blocker spadin (Fig. 4C) and the non-selective TREK-1 blocker quinine (Fig. 4D) reversed this effect. We next used the thalium assay to assess the effect of riluzole on $K^+$ flux in PC3 cells. We measured clear-cut increase in thalium flux when the cells were treated for 48 h with riluzole concentrations of 25 μM and above (Fig. 4E). This increase was lost when PC3 cells were co-treated with spadin (Fig. 4F), which per se did not have any effect (Suppl. Fig. 3C).

## 4. Discussion

Bone pain induced by prostate cancer metastases, as in other cancers having a bone tropism, is characterized by the development of pain triggered by movements and by spontaneous pain, which significantly contribute to deterioration of the patients' quality of life. We chose a mouse model of bone pain induced by intratibial injection of human PC3 prostate cancer cells as previously described [19]. This model results in localized tumor development with an uptake percentage of 100 %, which mimics the highest clinical stage existing in prostate cancer and allows easy evaluation of the painful symptoms induced by bone metastases in animals. In our conditions, pain developed 14 days after the injection of the cells. In agreement with previous reports [32], our results suggest that pain occurs early compared to the appearance of bone lysis.

Clinically, opioids are the only pharmacological treatment in humans with effectiveness against intense pain resulting from a malignant bone tumor. Unfortunately, however, their effectiveness is limited and many patients are left without adequate treatment. As in previous published data [21], we did not observe any analgesic effect of morphine at the dose used in our rodent model. Interestingly, and unlike morphine, riluzole resulted in relief until late stages of both evoked and spontaneous painful symptoms. This result is consistent with the already documented analgesic effects of riluzole in a number of inflammatory [16,19,33–35] and neuropathic pain models [13,15,33,36–38]. One important target of riluzole is the TREK-1 channel [12], a channel involved in both neuroprotection and analgesia [39]. The analgesic effects of riluzole were previously shown to be specifically dependent on the TREK-1 channel in a neuropathic pain model induced by the anticancer agent oxaliplatin [13]. Using a selective pharmacological strategy to block the channel, we also observed a TREK-1-dependent antinociceptive effect of this drug in bone cancer pain.

Because of the limited understanding of the mechanisms involved, few therapies have been developed that could control bone cancer pain without significant unwanted side effects. Besides its numerous adverse effects, morphine can also exacerbate osteolysis and consequently hypersensitivity [40]. Riluzole, recognized as a well-tolerated molecule after decades of treatments of ALS patients, did not induce bone loss nor did it affect bone remodeling in our model.

While the analgesic effect observed in a PCa animal model is very encouraging, the particular context of cancer patients nevertheless raises the question of the effect of riluzole on tumor progression. In agreement with data evidencing an antiproliferative effect of riluzole on numerous cancer cell lines [41–43], including androgen receptor (AR)-dependent and independent prostate cancer lines [28,44], we show that riluzole can decrease PC3 cell viability *in vitro*. Given the involvement of the TREK-1 channel in the beneficial effects of riluzole on pain in CIBP mice, we sought to determine whether the antiproliferative effect of riluzole on PC3 cells was also linked to the activation of the TREK-1 channel. Using the specific blocker spadin, we found that effect of riluzole on PC3 cell viability is lost when spadin is co-administered, suggesting that the activity of riluzole on these cancer cells is dependent on the TREK-1 channel. Those results are in line with the observation that another TREK-1 activator, BL1249, also inhibits pancreatic cancer cell proliferation and migration. The decrease in PC3 cell viability can be correlated with an increase in Vm measured in PC3 cells, involving, at least in part, an increase in TREK-1-mediated $K^+$ efflux that is TREK-1 dependent. Again, these results are concordant with observations indicating that highly proliferative tumor cells generally show a depolarized Vm, whereas quiescent cells are hyperpolarized [30,31].

In conclusion we show that riluzole, which is a very safe drug used in ALS, is also a compound that can be a serious contender for the treatment of pain in bone cancer patients. In addition, the antiproliferative effects of riluzole observed *in vitro* encourage the potential use of combined therapy with anticancer agents. The systematic involvement of TREK1 in these positive effects highlights the interest of this channel as a pharmacological target for analgesic drugs. This finding is to be seen in light of the growing interest of ion channels as a new target for both pain and cancer therapies [45,46].

## CRediT authorship contribution statement

**Mathilde Fereyrolles:** Investigation. **Julie Barbier:** Investigation, Formal analysis. **Youssef Aissouni:** Validation, Investigation, Formal analysis. **Laetitia Prival:** Investigation, Formal analysis. **Stephane Lolignier:** Writing – review & editing. **Sylvain Lamoine:** Methodology, Investigation, Formal analysis. **Jerome Busserolles:** Writing – review &

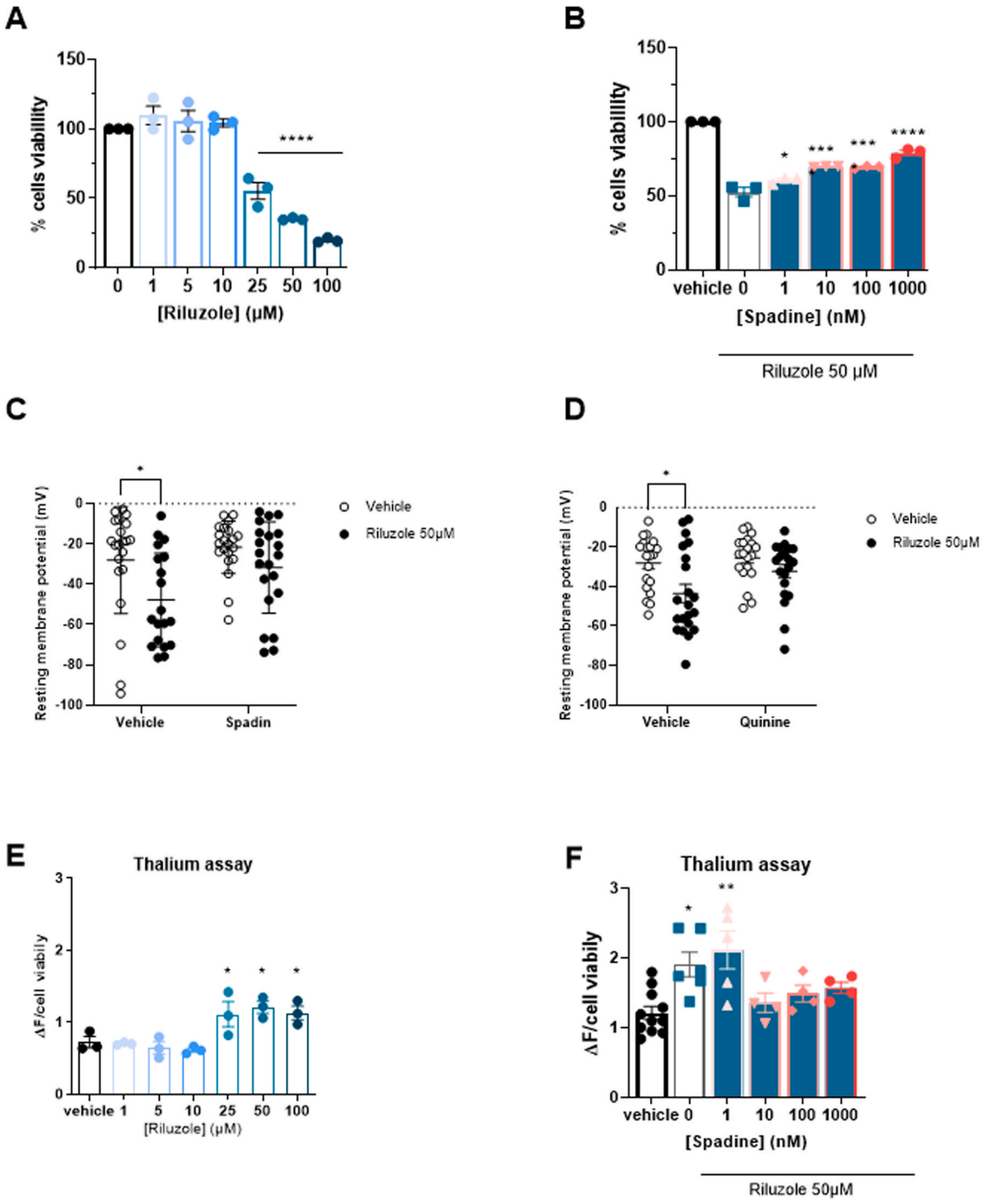


**Fig. 4. Riluzole decreases PC3 cell viability in vitro** (A) Riluzole dose-dependently (1–100 μM) inhibited the survival of PC3 cells as measured by inhibition of mitochondrial dehydrogenase activity (MTT assay). The average results from at least three independent experiments are presented. Values are expressed as mean ± SEM. Statistical analysis was performed with one-way ANOVA and Dunnett's multicomparison post-hoc test; *** $p < 0{,}001$, *versus* the vehicle group. (B) The effect of riluzole, used at 50 μM, on PC3 cell viability was dose-dependently blocked by spadin (1–1000 nM). The average results from at least three independent experiments are presented. Values are expressed as mean ± SEM. Statistical analysis was performed with one-way ANOVA and Dunnett's multicomparison post-hoc test; * $p < 0{,}05$, *** $p < 0.001$ *versus* the group treated with riluzole alone. (C) Vm was measured in PC3 cells using whole cell patch-clamp. The depolarized Vm measured in PC3 cells was hyperpolarized by riluzole treatment (48 h). The effect was prevented by co-treatment with the selective TREK-1 blocker spadin. (D) The non-selective TREK-1 blocker quinine also significantly prevented the effect of riluzole on PC3 Vm. (E) Riluzole (48 h treatment) significantly increased thallium flux in PC3 cells in the 25–100 μM concentration range. Statistical analysis was performed using one ANOVA with Dunnett's multicomparisons post-hoc test; * $p < 0{,}05$, *versus* the vehicle group. (F) Spadin (10–1000 nM) significantly blocked the effect of riluzole (50 μM) on thallium flux in PC3 cells. The average results from at least three independent experiments are presented. Values are expressed as mean ± SEM. Statistical analysis was performed using one ANOVA with Tukey's multicomparison post-hoc test; * $p < 0{,}05$, ** $p < 0.01$ *versus* the vehicle group.

editing, Writing – original draft, Supervision, Funding acquisition, Conceptualization. **Mathieu Meleine:** Investigation, Formal analysis. **Michel Lazdunski:** Writing – review & editing. **Alain Eschalier:** Writing – review & editing, Funding acquisition, Conceptualization. **Mélissa Delanne-Cumenal:** Writing – review & editing, Visualization, Investigation, Formal analysis. **Ludivine Boudieu:** Investigation. **Julien Schopp:** Investigation. **Christine Cercy:** Investigation.

## Declaration of Competing Interest

The authors declare that they have no known competing financial interests or personal relationships that could have appeared to influence the work reported in this paper.

## Acknowledgments

This project was funded by the University of Clermont Auvergne, the French government through the programme "Investissements d'Avenir" (I-Site CAP 20-25), the Société Française d'Etude et de Traitement de la Douleur, the Cancéropôle Lyon Auvergne Rhône-Alpes. All imaging experiments were carried out within the multimodal imaging platform IVIA (Clermont-Ferrand, France), by Pr E. Miot-Noirault, Dr Sophie Besse and Dr A Briat.

### *Conflict of interest statement*

The authors have declared that no conflict of interest exists.

## Appendix A. Supporting information

Supplementary data associated with this article can be found in the online version at doi:10.1016/j.biopha.2024.116887.

## References

[1] K.N. Weilbaecher, T.A. Guise, L.K. McCauley, Cancer to bone: a fatal attraction, Nat. Rev. Cancer 11 (2011) 411–425, https://doi.org/10.1038/nrc3055.
[2] J.M. Jimenez-Andrade, W.G. Mantyh, A.P. Bloom, A.S. Ferng, C.P. Geffre, P. W. Mantyh, Bone cancer pain: bone cancer pain, Ann. N. Y. Acad. Sci. 1198 (2010) 173–181, https://doi.org/10.1111/j.1749-6632.2009.05429.x.
[3] M. Fallon, R. Giusti, F. Aielli, P. Hoskin, R. Rolke, M. Sharma, C.I. Ripamonti, ESMO Guidelines Committee, Management of cancer pain in adult patients: ESMO clinical practice guidelines, Ann. Oncol. 29 (2018) iv166–iv191, https://doi.org/10.1093/annonc/mdy152.
[4] A. Caraceni, G. Hanks, S. Kaasa, M.I. Bennett, C. Brunelli, N. Cherny, O. Dale, F. De Conno, M. Fallon, M. Hanna, D.F. Haugen, G. Juhl, S. King, P. Klepstad, E. A. Laugsand, M. Maltoni, S. Mercadante, M. Nabal, A. Pigni, L. Radbruch, C. Reid, P. Sjogren, P.C. Stone, D. Tassinari, G. Zeppetella, Use of opioid analgesics in the treatment of cancer pain: evidence-based recommendations from the EAPC, Lancet Oncol. 13 (2012) e58–e68, https://doi.org/10.1016/S1470-2045(12)70040-2.
[5] J.A. Paice, K. Bohlke, D. Barton, D.S. Craig, A. El-Jawahri, D.L. Hershman, L. R. Kong, G.P. Kurita, T.W. LeBlanc, S. Mercadante, K.L.M. Novick, R. Sedhom, C. Seigel, J. Stimmel, E. Bruera, Use of opioids for adults with pain from cancer or cancer treatment: ASCO guideline, J. Clin. Oncol. 41 (2023) 914–930, https://doi.org/10.1200/JCO.22.02198.
[6] P.J. Wiffen, B. Wee, S. Derry, R.F. Bell, R.A. Moore, Opioids for cancer pain – an overview of Cochrane reviews, Cochrane Database Syst. Rev. 7 (2017) CD012592, https://doi.org/10.1002/14651858.CD012592.pub2.
[7] M. Devilliers, J. Busserolles, S. Lolignier, E. Deval, V. Pereira, A. Alloui, M. Christin, B. Mazet, P. Delmas, J. Noel, M. Lazdunski, A. Eschalier, Activation of TREK-1 by morphine results in analgesia without adverse side effects, Nat. Commun. 4 (2013) 2941, https://doi.org/10.1038/ncomms3941.
[8] F. Lesage, M. Lazdunski, Molecular and functional properties of two-pore-domain potassium channels, Am. J. Physiol. Ren. Physiol. 279 (2000) F793–F801, https://doi.org/10.1152/ajprenal.2000.279.5.F793.
[9] F. Maingret, I. Lauritzen, A.J. Patel, C. Heurteaux, R. Reyes, F. Lesage, M. Lazdunski, E. Honoré, TREK-1 is a heat-activated background K(+) channel, EMBO J. 19 (2000) 2483–2491, https://doi.org/10.1093/emboj/19.11.2483.
[10] A. Alloui, K. Zimmermann, J. Mamet, F. Duprat, J. Noël, J. Chemin, N. Guy, N. Blondeau, N. Voilley, C. Rubat-Coudert, M. Borsotto, G. Romey, C. Heurteaux, P. Reeh, A. Eschalier, M. Lazdunski, TREK-1, a K+ channel involved in polymodal pain perception, EMBO J. 25 (2006) 2368–2376, https://doi.org/10.1038/sj.emboj.7601116.
[11] J. Noël, K. Zimmermann, J. Busserolles, E. Deval, A. Alloui, S. Diochot, N. Guy, M. Borsotto, P. Reeh, A. Eschalier, M. Lazdunski, The mechano-activated K+ channels TRAAK and TREK-1 control both warm and cold perception, EMBO J. 28 (2009) 1308–1318, https://doi.org/10.1038/emboj.2009.57.
[12] F. Duprat, F. Lesage, A.J. Patel, M. Fink, G. Romey, M. Lazdunski, The neuroprotective agent riluzole activates the two P domain K(+) channels TREK-1 and TRAAK, Mol. Pharm. 57 (2000) 906–912.
[13] L. Poupon, S. Lamoine, V. Pereira, D.A. Barriere, S. Lolignier, F. Giraudet, Y. Aissouni, M. Meleine, L. Prival, D. Richard, N. Kerckhove, N. Authier, D. Balayssac, A. Eschalier, M. Lazdunski, J. Busserolles, Targeting the TREK-1 potassium channel via riluzole to eliminate the neuropathic and depressive-like effects of oxaliplatin, Neuropharmacology 140 (2018) 43–61, https://doi.org/10.1016/j.neuropharm.2018.07.026.
[14] E.S. Moon, S.K. Karadimas, W.-R. Yu, J.W. Austin, M.G. Fehlings, Riluzole attenuates neuropathic pain and enhances functional recovery in a rodent model of cervical spondylotic myelopathy, Neurobiol. Dis. 62 (2014) 394–406, https://doi.org/10.1016/j.nbd.2013.10.020.
[15] A. Hama, J. Sagen, Antinociceptive effect of riluzole in rats with neuropathic spinal cord injury pain, J. Neurotrauma 28 (2011) 127–134, https://doi.org/10.1089/neu.2010.1539.
[16] G. Munro, H. Erichsen, N. Mirza, Pharmacological comparison of anticonvulsant drugs in animal models of persistent pain and anxiety, Neuropharmacology 53 (2007) 609–618, https://doi.org/10.1016/j.neuropharm.2007.07.002.
[17] G. Blackburn-Munro, N. Ibsen, H.K. Erichsen, A comparison of the anti-nociceptive effects of voltage-activated Na+ channel blockers in the formalin test, Eur. J. Pharm. 445 (2002) 231–238, https://doi.org/10.1016/S0014-2999(02)01765-X.
[18] A. Blyufer, S. Lhamo, C. Tam, I. Tariq, T. Thavornwatanayong, S. Mahajan, Riluzole: a neuroprotective drug with potential as a novel anti-cancer agent (review), Int. J. Oncol. 59 (2021), https://doi.org/10.3892/ijo.2021.5275.
[19] A. Fradet, H. Sorel, B. Depalle, C.M. Serre, D. Farlay, A. Turtoi, A. Bellahcene, H. Follet, V. Castronovo, P. Clézardin, E. Bonnelye, A new murine model of osteoblastic/osteolytic lesions from human androgen-resistant prostate cancer, PLoS One 8 (2013) e75092, https://doi.org/10.1371/journal.pone.0075092.
[20] S. Reagan-Shaw, M. Nihal, N. Ahmad, Dose translation from animal to human studies revisited, FASEB J. 22 (2008) 659–661, https://doi.org/10.1096/fj.07-9574LSF.
[21] N.M. Luger, M.A.C. Sabino, M.J. Schwei, D.B. Mach, J.D. Pomonis, C.P. Keyser, M. Rathbun, D.R. Clohisy, P. Honore, T.L. Yaksh, P.W. Mantyh, Efficacy of systemic morphine suggests a fundamental difference in the mechanisms that generate bone cancer vs. inflammatory pain, Pain 99 (2002) 397–406, https://doi.org/10.1016/S0304-3959(02)00102-1.
[22] C. Zhu, J. Tang, T. Ding, L. Chen, W. Wang, X.-P. Mei, X.-T. He, W. Wang, L.-D. Zhang, Y.-L. Dong, Z.-J. Luo, Neuron-restrictive silencer factor-mediated downregulation of μ-opioid receptor contributes to the reduced morphine analgesia in bone cancer pain, Pain 158 (2017) 879–890, https://doi.org/10.1097/j.pain.0000000000000848.
[23] J. Busserolles, I. Ben Soussia, L. Pouchol, N. Marie, M. Meleine, M. Devilliers, C. Judon, J. Schopp, L. Clémenceau, L. Poupon, E. Chapuy, S. Richard, F. Noble, F. Lesage, S. Ducki, A. Eschalier, S. Lolignier, TREK1 channel activation as a new analgesic strategy devoid of opioid adverse effects, Br. J. Pharm. 177 (2020) 4782–4795, https://doi.org/10.1111/bph.15243.
[24] G.D. Roodman, Mechanisms of bone metastasis, N. Engl. J. Med. 350 (2004) 1655–1664, https://doi.org/10.1056/NEJMra030831.
[25] S. Hughes, J. Magnay, M. Foreman, S.J. Publicover, J.P. Dobson, A.J. El Haj, Expression of the mechanosensitive 2PK+ channel TREK-1 in human osteoblasts, J. Cell. Physiol. 206 (2006) 738–748, https://doi.org/10.1002/jcp.20536.
[26] H. Moha Ou Maati, J. Veyssiere, F. Labbal, T. Coppola, C. Gandin, C. Widmann, J. Mazella, C. Heurteaux, M. Borsotto, Spadin as a new antidepressant: absence of TREK-1-related side effects, Neuropharmacology 62 (2012) 278–288, https://doi.org/10.1016/j.neuropharm.2011.07.019.
[27] N. Rizaner, S. Uzun, S.P. Fraser, M.B.A. Djamgoz, S. Altun, Riluzole: anti-invasive effects on rat prostate cancer cells under normoxic and hypoxic conditions, Basic Clin. Pharm. Toxicol. 127 (2020) 254–264, https://doi.org/10.1111/bcpt.13417.
[28] K.M. Wadosky, M. Shourideh, D.W. Goodrich, S. Koochekpour, Riluzole induces AR degradation via endoplasmic reticulum stress pathway in androgen-dependent and castration-resistant prostate cancer cells, Prostate 79 (2019) 140–150, https://doi.org/10.1002/pros.23719.
[29] K. Akamatsu, M.-A. Shibata, Y. Ito, Y. Sohma, H. Azuma, Y. Otsuki, Riluzole induces apoptotic cell death in human prostate cancer cells via endoplasmic reticulum stress, Anticancer Res. 29 (2009) 2195–2204.
[30] C.D. Cone, Unified theory on the basic mechanism of normal mitotic control and oncogenesis, J. Theor. Biol. 30 (1971) 151–181, https://doi.org/10.1016/0022-5193(71)90042-7.
[31] M. Yang, W.J. Brackenbury, Membrane potential and cancer progression, Front. Physiol. 4 (2013), https://doi.org/10.3389/fphys.2013.00185.
[32] M.L. Thompson, J.M. Jimenez-Andrade, S. Chartier, J. Tsai, E.A. Burton, G. Habets, P.S. Lin, B.L. West, P.W. Mantyh, Targeting cells of the myeloid lineage attenuates pain and disease progression in a prostate model of bone cancer, Pain 156 (2015) 1692–1702, https://doi.org/10.1097/j.pain.0000000000000228.
[33] T.J. Coderre, N. Kumar, C.D. Lefebvre, J.S.C. Yu, A comparison of the glutamate release inhibition and anti-allodynic effects of gabapentin, lamotrigine, and riluzole in a model of neuropathic pain, J. Neurochem. 100 (2007) 1289–1299, https://doi.org/10.1111/j.1471-4159.2006.04304.x.
[34] J.M. Thompson, G. Ji, V. Neugebauer, Small-conductance calcium-activated potassium (SK) channels in the amygdala mediate pain-inhibiting effects of clinically available riluzole in a rat model of arthritis pain, Mol. Pain 11 (2015) s12990-015-0055, https://doi.org/10.1186/s12990-015-0055-9.

[35] C. Abarca, E. Silva, M.J. Sepúlveda, P. Oliva, E. Contreras, Neurochemical changes after morphine, dizocilpine or riluzole in the ventral posterolateral thalamic nuclei of rats with hyperalgesia, Eur. J. Pharm. 403 (2000) 67–74, https://doi.org/10.1016/S0014-2999(00)00502-1.

[36] B. Sung, G. Lim, J. Mao, Altered expression and uptake activity of spinal glutamate transporters after nerve injury contribute to the pathogenesis of neuropathic pain in rats, J. Neurosci. 23 (2003) 2899–2910, https://doi.org/10.1523/JNEUROSCI.23-07-02899.2003.

[37] D.J. Chew, T. Carlstedt, P.J. Shortland, The effects of minocycline or riluzole treatment on spinal root avulsion–induced pain in adult rats, J. Pain 15 (2014) 664–675, https://doi.org/10.1016/j.jpain.2014.03.001.

[38] K. Jiang, Y. Zhuang, M. Yan, H. Chen, A.-Q. Ge, L. Sun, B. Miao, Effects of riluzole on P2×7R expression in the spinal cord in rat model of neuropathic pain, Neurosci. Lett. 618 (2016) 127–133, https://doi.org/10.1016/j.neulet.2016.02.065.

[39] D.A. Bayliss, P.Q. Barrett, Emerging roles for two-pore-domain potassium channels and their potential therapeutic impact, Trends Pharm. Sci. 29 (2008) 566–575, https://doi.org/10.1016/j.tips.2008.07.013.

[40] A.L. Thompson, S.A. Grenald, H.A. Ciccone, D. Mohty, A.F. Smith, D.L. Coleman, E. Bahramnejad, E. De Leon, L. Kasper-Conella, J.L. Uhrlab, D.S. Margolis, D. Salvemini, T.M. Largent-Milnes, T.W. Vanderah, Morphine-induced osteolysis and hypersensitivity is mediated through toll-like receptor-4 in a murine model of metastatic breast cancer, Pain 164 (2023) 2463–2476, https://doi.org/10.1097/j.pain.0000000000002953.

[41] S. Liao, Y. Ruiz, H. Gulzar, Z. Yelskaya, L. Ait Taouit, M. Houssou, T. Jaikaran, Y. Schvarts, K. Kozlitina, U. Basu-Roy, A. Mansukhani, S.S. Mahajan, Osteosarcoma cell proliferation and survival requires mGluR5 receptor activity and is blocked by Riluzole, PLoS One 12 (2017) e0171256, https://doi.org/10.1371/journal.pone.0171256.

[42] C.L. Speyer, J.S. Smith, M. Banda, J.A. DeVries, T. Mekani, D.H. Gorski, Metabotropic glutamate receptor-1: a potential therapeutic target for the treatment of breast cancer, Breast Cancer Res. Treat. 132 (2012) 565–573, https://doi.org/10.1007/s10549-011-1624-x.

[43] C. Zhang, X. Yuan, H. Li, Z. Zhao, Y. Liao, X. Wang, J. Su, S. Sang, Q. Liu, Anti-cancer effect of metabotropic glutamate receptor 1 inhibition in human glioma U87 cells: involvement of PI3K/Akt/mTOR pathway, Cell. Physiol. Biochem. 35 (2015) 419–432, https://doi.org/10.1159/000369707.

[44] S. Koochekpour, S. Majumdar, G. Azabdaftari, K. Attwood, R. Scioneaux, D. Subramani, C. Manhardt, G.D. Lorusso, S.S. Willard, H. Thompson, M. Shourideh, K. Rezaei, O. Sartor, J.L. Mohler, R.L. Vessella, Serum glutamate levels correlate with Gleason score and glutamate blockade decreases proliferation, migration, and invasion and induces apoptosis in prostate cancer cells, Clin. Cancer Res. 18 (2012) 5888–5901, https://doi.org/10.1158/1078-0432.CCR-12-1308.

[45] L.A. Pardo, W. Stühmer, The roles of K(+) channels in cancer, Nat. Rev. Cancer 14 (2014) 39–48, https://doi.org/10.1038/nrc3635.

[46] P. Enyedi, G. Czirják, Molecular background of leak K+ currents: two-pore domain potassium channels, Physiol. Rev. 90 (2010) 559–605, https://doi.org/10.1152/physrev.00029.2009.